Redispersible Hybrid Nanopowders: Cerium Oxide Nanoparticle Complexes with Phosphonated-PEG Oligomers.

L. Qi*, A. Sehgal*, J.-C. Castaing*, J. Fresnais**, J.-F. Berret**, J.-P. Chapel*

*Complex Fluid Laboratory, CRTB Rhodia Inc., Bristol, PA 19007, USA.
**Matière et Systèmes Complexes, Université Denis Diderot (Paris 7), F-75205 Paris, France.

ABSTRACT

Rare earth cerium oxide (ceria) nanoparticles are stabilized using end-functional phosphonated-PEG oligomers. The final structure of the resulting hybrid core-shell singlet nanocolloids is characterized and modeled using light and neutron scattering data. The adsorption mechanism is non-stoichiometric with a high affinity adsorption isotherm. This solvating brush-like layer is sufficient to solubilize the particles and greatly expand the stability range to pH=9. The final tailored sol not only maintains the original strong UV absorption capability but also possesses supplementary attributes relating to the presence of PEG layer, such as redispersibility in aqueous or organic solvents after freeze-drying and tunable interfacial properties which are essential for surface modification, Pickering emulsions or supracolloidal assemblies. This *robust* platform enables translation of intrinsic properties of mineral oxide nanoparticles to critical end use.

***Keywords*:** nanoparticle, cerium oxide, phosphonated-PEG, redispersible, interfacial activity

1 INTRODUCTION

The size–dependent properties of nanoparticles have generated diverse scientific interests. The primary limitation of inorganic nanosol stability to physico-chemical perturbation from their "as synthesized" state during processing represents the critical challenge for any given application. The need to offset the attractive *van der Waals* interaction has been addressed through the adsorption of an organic layer around the particle promoting an electro-steric or steric stabilization of the sol. In addition to stabilization, the organic shell and/or the presence of some specific groups in the corona may also confer some functionality to the high surface area of the nanoparticles. Surface derivatization is crucial in biomedical applications.

We report a facile complexation process giving rise to robust and versatile hybrid metal oxide nanoparticle sols with a well anchored neutral corona for wide applicability. It has been shown that phosphonic acid groups bind strongly to a variety of metal oxide surfaces at room temperature in aqueous solution [1]. We also chose PEG groups that are widely used in biomedical applications to prevent non-specific adsorption of proteins. Cerium oxide nanocrystals, or nanoceria is chosen to illustrate this approach due to its growing importance in science and technology ranging from material science (catalysis, polishing, optics…) [2] to biomedical [3] applications.

In the following section, we describe, characterize and model the complexation process and the resulting nanostructure of the hybrid particles. We underscore three key attributes of the tailored sol: i) strong *UV absorption* capability, ii) ability to *re-disperse* after freeze-drying as powder in *aqueous or organic solvents* as singlet nanocolloids and iii) tunable interfacial properties via PEG structure tailoring.

2 MATERIALS AND METHODES

2.1 Oligomers and Nanoparticles

The nanoceria consisted of isotropic agglomerates of 2-5 crystallites with a typical size of 2 nm and faceted morphologies. Their average radius determined by cryogenic transmission electron microscopy (cryo-TEM) amounts to 7 nm, with a polydispersity of 0.15. As synthesized, the cerium oxide nanosols are stabilized by combination of long range electrostatic forces and short range hydration interactions at pH 1.5. An increase of the pH *or* ionic strength (>0.45 M) results in a reversible aggregation of the particles, leading eventually to a macroscopic phase separation. The destabilization of the sols occurs well below the point of zero charge of the ceria particles, pzc=7.9 [4]. The bare nanoceria particles have a zeta potential ζ = +30 mV and an estimated structural charge of Q_{CeO_2} = +300 e.

The phosphonate-PEG oligomers investigated in this work include a 3-phosphonopropyl alcohol ethoxylate-10 EO) and a 3-phosphonopropyl alcohol ethoxylate cetyl-10EO, both produced by *Rhodia Inc.* and named hereafter respectively PPEG and hydrophobic sticker. Titration curves with NaOH (1M) show the presence of two distinct p*K*as for PPEG at pKa_1 = 2.7 and pKa_2 = 7.8. The critical

micellization concentration (CMC) of hydrophobic stickers was found to be between 0.05mM and 0.1mM in pure water (light scattering), and at 7.3mM in a mixture of ethanol/water (50/50 vol/vol) (conductivity measurements).

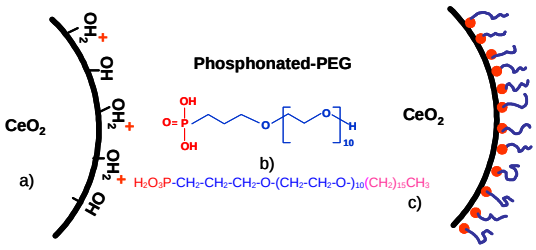

Figure 1 : (a) Simplified sketch of the surface chemistry of cerium oxide nanoparticles: cationic protonated hydroxyl groups versus neutral hydroxyl groups. (b) Tailored PPEG chemical architectures for the adsorption onto nanoparticles (c) PPEG corona around the particle: steric stabilization + PEG functionality.

2.2 Hybrid Nanoparticles Formulation

The pH of the PPEG solution (pure or with hydrophobic sticker unimers) is adjusted with reagent-grade nitric acid (HNO_3) to 1.5. Mixed solutions of nanoparticles (CeO_2) and PPEG are prepared by simple mixing of dilute solutions prepared at the same concentration c (c = 0.1 - 1 wt. %) and same pH. The relative amount of each component is monitored by the volume ratio X, yielding for the final concentrations:

$$c_{CeO_2} = \frac{cX}{1+X} \quad , \; c_{\text{oligomer}} = \frac{c}{1+X} \qquad (1)$$

Ammonium hydroxide (NH_4OH) is used to adjust the pH of CeO_2-PPEG dispersions in the range of 1.5 to 10.

3 RESULTS AND DISCUSSION

3.1 Light Scattering

Static and dynamic light scattering (SLS and DLS) was used to investigate the microstructure and stability of the electrostatic complexes in bulk solutions. With an overall concentration c kept constant, the Rayleigh ratios and hydrodynamic diameters are measured and plotted versus the mixing ratio X (Figure 3). $X=10^{-4}$ corresponds to a solution containing only PPEG oligomers and X=1000 corresponds to a solution containing only bare nanoceria particles. When X decreases from 1000 to 0.01, the size of the coated nanoceria increases gradually up to a critical value noted X_p where it then saturates around D_H = 13 nm. We interpret this result as the progressive coating of the particles by the oligomers until full coverage occurring at X_p, which can be fitted with a non-stoichiometric adsorption model (NST) (Figure 2). Below the critical volume ratio X_p, the particles are fully covered and in equilibrium with a decreasing number of non-absorbed oligomers. Above X_p, the number of grafted oligomers progressively decreases toward bare particles (X = ∞). At X_p, all the oligomers present in the initial solution are adsorbed onto the particle. The normalized Rayleigh ratio (normalization by the Rayleigh ratio of the bare nanoceria R_{NP} (X=∞)), as measured by SLS, is also monitored as a function of X. Here as well, one can clearly identify a critical ratio X equal to X_p where the Rayleigh ratio starts to decrease progressively with X. We interpret this result as the dilution of the fully covered particles by the free oligomers present in the bulk, in agreement with DLS results.

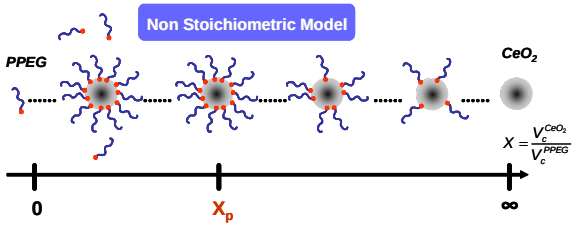

Figure 2. Schematic representation for the non-stoichiometric adsorption mechanism of PPEG onto nanoceria particles.

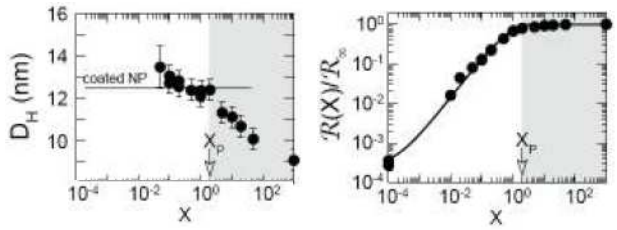

Figure 3. Rayleigh ratio and hydrodynamic radius D_H vs. X at low pH (pH=1.5). The continuous line is a fit to the data using a non-stoichiometric model for adsorption

3.2 Neutron Scattering

Neutron scattering is performed in H_2O and D_2O for the CeO_2 and PPEG-CeO_2 system respectively. Figure 4 shows the form factor of both bare and modified particles. The extra contribution to the scattered intensity due to the presence of the organic layer is clearly seen at low q in the Guinier representation where $R_g q < 1$ (inset Figure 4), where we can deduce a radius of gyration R_g = 3.2 ± 0.1 nm for the bare nanoparticles and R_g = 4.4 ± 0.1 nm for the PPEG coated ones.

3.3 Adsorption Isotherms

In order to evaluate the affinity of the PPEG oligomers with the surface of cerium oxide nanoparticles, adsorption isotherms are measured on macroscopically flat CeO_2 model surfaces with the help of optical reflectometry. As seen in Figure 5, at both investigated pH**,** the curves present a rather sharp increase of the adsorbed amount at very low

NSTI-Nanotech 2008, www.nsti.org, ISBN 978-1-4200-8504-4 Vol. 2

concentration. This rapid flattening out of the adsorbed amount suggests a rather high affinity of the oligomers toward cerium oxide surface.

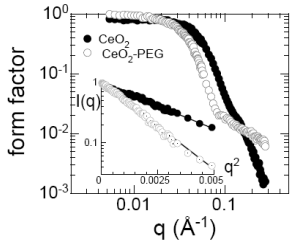

Figure 4. SANS form factor P (q) for bare and coated nanoparticles. Inset: Guinier representation of the intensity for the same samples (I(q) versus q^2).

The data of Figure 5 can be fitted using a Langmuir [4] model and the adsorption free energies ΔG^{ads} are found to be -16 k_BT and -15.8 k_BT for pH=1.5 and pH=6.5 respectively. Though the exact nature of the bond between PPEG and ceria is not known at this stage, the measured free energies might indicate an adsorption mechanism controlled by electrostatic interaction [5].

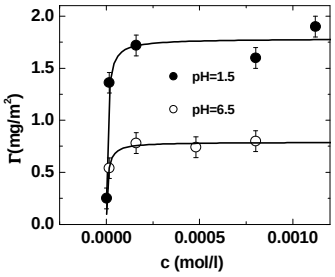

Figure 5. Adsorption isotherms of PPEG oligomers onto model CeO_2-coated substrates at low (1.5) and neutral pH (6). The solid curve is the Langmuir fit to the data.

3.4 Redispersible Nanopowders

Bare and hybrid nanoceria solutions were freeze-dried then re-dispersed in aqueous solutions at pH=1.5 for bare particles and DI water for stabilized particles and stirred overnight. Figure 6 shows the correlation functions measured with DLS (at 90º) of the original and modified sol before and after re-dispersion. The distributions P(D) of the hydration diameters D_H are also shown (inset Figure 6). After re-dispersion, the correlation function of the bare CeO_2 solution is clearly shifted toward longer times. As a result, the mean D_H is shifted toward larger values together with a clear broadening of the distribution compared to that of the original solution. In the case of *passivated* PPEG-CeO_2 particles, the freeze-drying process did not significantly change the original distribution indicating no change in the surface complexation of PPEG during the drying process. This has clear implications for the utility of nanoceria providing cost and processing advantages. In addition, the hybrid metal oxide powder is *also re-dispersible in certain organic solvents* like ethanol, acetone or chloroform which is not the case for bare particles.

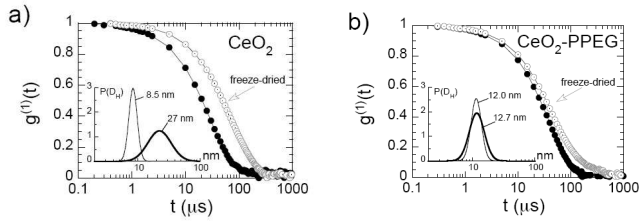

Figure 6. Re-dispersion in aqueous solutions of CeO_2 and PPEG-CeO_2 powders obtained by freeze-drying both stock solutions. a) original sol before and after freeze-drying and re-dispersion. b) id. hybrid sol. ($X < X_p$)

The complexation of nanoceria with end-functional PPEG to create true redispersible nanopowders in aqueous or certain organic solvents provides the framework for designing a truly versatile hybrid metal oxide sol with clear utility in a range of applications. Finally, UV-visible measurements have shown that the presence of the organic layer does not affect (via possible metal-ligands charge transfer complexes) the well known UV absorbance properties of bare particles. This result has direct impact for applications where anti-UV protection is needed.

3.6 Tunable interfacial properties

Pendant drop experiments performed on diluted (0.1% wt) aqueous solutions of nanoparticles show that the presence of the PEG shell confers some interfacial activity to the original nanoparticles, as can be seen in Figure 4. The bare charged CeO_2 nanoparticles do not adsorb to air/water interface (slight depletion likely due to image forces); while functionalized nanoparticles do adsorb, reducing the interfacial energy in agreement with the known PEG surface pressure (~10mn/m); with a small fraction (1% wt) of hydrophobic sticker added during the formulation, the surface tension is further reduced highlighting the possibility of tuning the interfacial energy via stickers content. Due to their surface activity, monolayers are formed at the air/water interface of a Langmuir trough enabling the formation of multilayers onto solid surfaces as seen in Figure10.

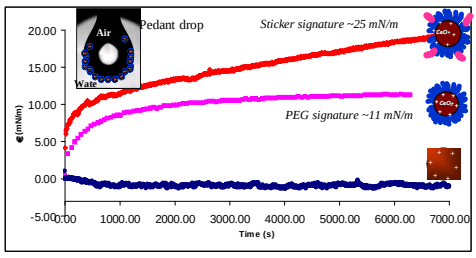

Figure 9. Pendant drop measurements monitor the evolution of the interfacial pressure $\pi = \gamma_{wate/air} - \gamma_{solutoin/air}$.

PEG functionalized nanoparticles were also shown to be good Pickering emulsion agents as seen in Figure 11, inhibiting the coalescence of the (water/hexadecane) emulsion droplets. Compared to micron-sized particles, nanoparticles display a constant particle exchange at the interface, leading the nanoparticle assembly to attain its equilibrium [6].

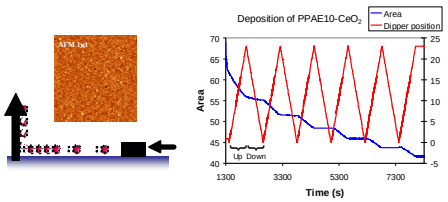

Figure 10. Multilayer of PEG-functionalized nanoceria via Langmuir-Blodgett deposition at pressure of 20 mn/m Monolayers transfer was certified by the variation of the trough area during deposition and via thickness measurements (ellipsometry).

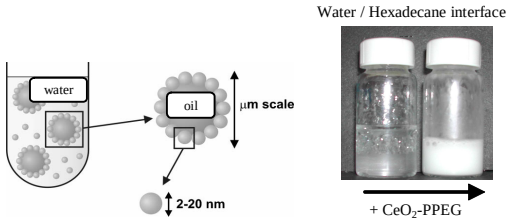

Figure 11. Picker emulsion of water/hexadecane by adding PEG functionalized nanoceria (partially reprinted from [6]).

For hybrid nanoparticles with a small fraction of hydrophobic stickers, it is shown that their interaction can be tuned by via the solvent surface tension.

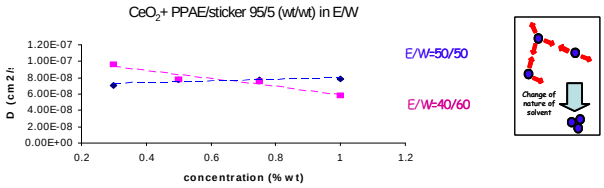

Figure 12. Mutual diffusion coefficient D vs. nanoparticle concentration c in ethanol/water mixtures.

DLS experiments were performed on PPEG/stickers (95/5 wt/wt) functionalized nanoceria. The evolution of the mutual diffusion coefficient D vs concentration c was plotted in Figure 12. It can be seen that at higher ethanol content (E/W=50/50), the second virial coefficient A_2 (~ slope of D vs. c) is positive indicating a slight repulsion between the particles; at lower ethanol content (E/W=40/60), A_2 becomes negative suggesting a slight attraction. In the latter case the steric repulsion provided by the PEG chains is balanced by a larger hydrophobic (attractive) interaction provided by the stickers. This simple route can likely be used to create supracolloidals assemblies. Their affinity for hydrophobic solid surfaces was further evaluated by reflectometry. It is shown in Figure 13 that the presence of a small quantity of stickers in the shell can double the adsorbed amount onto a polystyrene surface

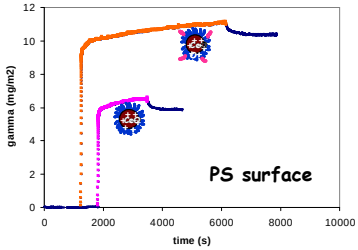

Figure 13. Adsorption of PPEG/stickers (99/1 wt/wt) functionalized nanoparticles onto PS surfaces monitored by optical reflectometry.

4 CONCLUSIONS

The generation of robust and versatile phosphonated-PEG cerium oxide nanoparticles is highlighted through a detailed series of complementary experiments. From quantitative light and neutron scattering data we are able to obtain the main features of the CeO_2-PPEG hybrid core-shell nanostructure and to model the adsorption mechanism. The NST model evidenced the presence of a critical ratio X_p at which the particles are fully covered. Beyond that threshold, the organic coating progressively diminishes, increasing the sensitiveness of the sol toward destabilization. In addition, the measurement of the free energy of adsorption ΔG^{ads} has shown that electrostatic interaction is likely the main driving force the complexation. This solvating brush-like layer is sufficient to solubilize the particles and greatly expands the stability range of the original sol up to pH=9. After functionalization, the particles maintain a strong UV absorption capability. Moreover, after freeze-drying, the hybrid particle powder was able to *re-disperse* in different solvents without losing any of its features conferring a great versatility and ease of use of the CeO_2-PPEG nanoparticles in dry or wet conditions. Beside their bulk properties, the hybrid nanoparticles present some very interesting interfacial properties which are tunable via the tailoring of the PEG structure. These results highlight the specificity of the terminus phosphonate group to create a robust and very versatile metal oxide hybrid sol.

5 REFERENCES

[1] a. Traina, C. A.; Schwartz, J. Langmuir 23, 9158, 2007 b. Gawalt, E. S. *et al.* Langmuir 19, 200, 2003.
[2] a.Yu, T. Z. et al. Solid-State Electron. 51, 894, 2007. b. Patsalas, P. *et al.* Appl. Phys. Lett. 81, 466, 2002. c. Feng, X. D. et al. Science 312, 1504, 2006.
[3] a. Tarnuzzer, R. *et al.* Nano Lett. 5, 2573, 2007. b. Chen, J. P.; Patil, S.; Seal, S.; McGinnis, J. F. Nat. Nanotechnol.1, 142, 2006.
[4] Nabavi M. *et al.* J. Coll. Int. Sci. 160, 459, 1993.
[5] Studart, A. R. *et al.* Langmuir, 23, 1081, 2007.
[6] Bouker A. *et al.* Soft Matter 3, 231, 2007.